The effect of a superconducting surface layer on the optical properties of a dielectric photonic composite

2008 J. Phys.: Condens. Matter 20 145203

(http://iopscience.iop.org/0953-8984/20/14/145203)

IOP Publishing Journal of Physics: Condensed Matter

J. Phys.: Condens. Matter **20** (2008) 145203 (15pp) doi:10.1088/0953-8984/20/14/145203

The effect of a superconducting surface layer on the optical properties of a dielectric photonic composite

H Rauh[1] **and Y A Genenko**

Institut für Materialwissenschaft, Technische Universität Darmstadt, 64287 Darmstadt, Germany

E-mail: hera@tgm.tu-darmstadt.de

Received 6 September 2007, in final form 29 November 2007
Published 18 March 2008
Online at stacks.iop.org/JPhysCM/20/145203

Abstract

The effect of a strongly anisotropic superconducting surface layer on the transmittance, reflectance and absorptance of a one-dimensional, layered dielectric composite with periodically alternating, isotropic constituents for linearly polarized, normally incident electromagnetic radiation is studied both analytically and numerically. The underlying model of the electric permittivity of the superconducting constituent permits photonic excitation at frequencies both below and above the superconductor pair breaking frequency as well as thermal and normal scattering right up to the superconductor critical temperature. The optical properties addressed reveal traits such as band-like patterns of the transmittance and reflectance, but also step-like or smeared-out patterns of the reflectance and absorptance, displaying a marked reference to the particular type of polarization by virtue of the anisotropy of the superconducting layer covering the dielectric composite. Thus, in switching from transverse electric to transverse magnetic polarization, the maximum optical selectivity can become gigantic, given an appropriate thickness of the superconducting layer, with a moderate dependence on temperature. This fact offers unique possibilities regarding practical applications of such a novel photonic composite as an efficient polarization filter for electromagnetic radiation tunable via the thickness of the covering layer and temperature.

1. Introduction

The interaction between electromagnetic radiation and matter is amongst the most fundamental sources of dynamics in nature; it brings about phenomena like the absorption and emission of photons or the scattering of light. Despite its fundamental character, this interaction can be controlled by means of photonic crystals, i.e. regularly structured, synthetic composites made up of materials with different refractive indices [1–4]. Such composites exhibit unique optical properties—selective transmission of electromagnetic waves in definite ranges of frequency perhaps being the most prominent of them—which offer ready exploitation for modern photonics and optoelectronics applications.

During the past two decades, great attention has been directed towards photonic crystals built from conventional dielectrics, either in pure form or in combination with normal metallic constituents. Of particular interest, however, are constituents able to undergo phase transitions from ordered states, since they display significantly different optical properties below and at the respective critical temperatures. Therefore, photonic crystals with ferroelectric [5, 6] or ferromagnetic [7, 8] constituents have been investigated recently. The use of these materials unfolds the added vista of controlling the optical properties of photonic structures by the imposition of electric or, respectively, magnetic fields. Superconductors, which show the said kind of phase transition too, represent another important class of materials in view of promising technological device applications. The sensitivity of their optical properties to the particular, superconducting or normal state has provoked copious ideas for the implementation of superconductors into photonic structures, e.g. as constituents of one- or two-dimensional composites [9–20], (a) emphasizing the

[1] Author to whom any correspondence should be addressed.

possibility of tuning the gaps between photonic bands [12, 13], and hence calibrating transmittances [14, 15], by virtue of superconducting elements, (b) examining the concept of an Abrikosov vortex lattice to act as a two-dimensional photonic crystal maintained through an external magnetic field [16], or (c) employing these artificial structures as metamaterials for observing effects of negative refraction at finite radiation frequencies [17, 18]. Further applications derive from the use of superconductor thin films for constructing band-stop filters [21, 22] and from the realization of lattices of superconductor cubes or plates for obtaining metamaterials at zero frequency [23].

Motivated by the potential for strongly modifying the optical properties of photonic crystals that planar defects reveal [24–28], we here study the effect of a superconducting surface layer on the transmittance, reflectance and absorptance of a regularly structured, one-dimensional dielectric composite. Unlike previous theoretical work analysing superconductor constituents, with its limitations to electromagnetic isotropy, small radiation frequencies and low temperatures, ours accounts for electromagnetic anisotropy, photonic excitation at arbitrary frequencies as well as thermal excitation and normal scattering right up to the superconductor critical temperature. Clearly, a surface layer of distinct crystallographic anisotropy terminating an otherwise isotropic dielectric composite will give rise to substantial discriminations of these optical properties depending on the polarization of the incident radiation; a fact which enables applications of such a novel photonic composite as an efficient polarization filter tunable via the thickness of the layer and temperature.

In section 2 we set out the general framework for describing propagation of the electromagnetic radiation and the flow of electromagnetic energy by means of the convenient vector potential approach. Applying this, in section 3 we introduce the photonic modes and pertinent bands of the dielectric composite, assuming linearly polarized radiation at normal incidence, and employ both for theoretically determining the optical properties addressed with or without the superconducting surface layer present. In section 4 we show numerical results of these properties for an epitaxial surface layer of a cuprate superconductor and perovskite dielectric constituents, examining two different layer thicknesses and three characteristic temperatures, and compare the results obtained with those prevailing when the surface layer were absent. Finally, in section 5 we conclude by summarizing the insights and results obtained, suggesting potential applications of the novel photonic composite. Details of the model of the tensor of electric permittivity of a superconductor established for the characterization of the surface layer and used in our calculations can be found in the appendix.

2. General framework

We proceed from the Maxwell equations for the electric field $\boldsymbol{E}$, magnetic field $\boldsymbol{H}$ and electric displacement $\boldsymbol{D}$ of the electromagnetic radiation at position $\boldsymbol{r}$ and time t propagating through a vacuum space or, respectively, a non-magnetic composite in the absence of free charges and static fields:

$$\nabla \times \boldsymbol{E} + \frac{1}{c}\frac{\partial \boldsymbol{H}}{\partial t} = 0 \tag{1}$$

and

$$\nabla \times \boldsymbol{H} - \frac{1}{c}\frac{\partial \boldsymbol{D}}{\partial t} = 0, \tag{2}$$

with c meaning the vacuum speed of light; furthermore

$$\nabla \cdot \boldsymbol{H} = 0 \tag{3}$$

and

$$\nabla \cdot \boldsymbol{D} = 0. \tag{4}$$

Any constituent of the composite is meant to be characterized by a linear relation of the sort

$$\boldsymbol{D} = \underline{\underline{\varepsilon}}\boldsymbol{E}, \tag{5}$$

where $\underline{\underline{\varepsilon}}$ denotes the respective tensor of electric permittivity subsuming, in general, effects of both electric polarization and electric current flow for temporally steady excitations.

The homogeneity of equations (1)–(4) admits the convenient introduction of a vector potential $\boldsymbol{A}$ as a single auxiliary function of $\boldsymbol{r}$ and t to yield the representation of the magnetic field

$$\boldsymbol{H} = \nabla \times \boldsymbol{A}. \tag{6}$$

With this choice, equation (3) is satisfied identically, and equation (1) yields the representation of the electric field,

$$\boldsymbol{E} = -\frac{1}{c}\frac{\partial \boldsymbol{A}}{\partial t}, \tag{7}$$

upon supplementing with the condition ('Coulomb gauge') [29]

$$\nabla \cdot \boldsymbol{A} = 0. \tag{8}$$

Substitution of equations (5)–(7) into equation (2) results in the equation of motion for $\boldsymbol{A}$:

$$\nabla \times (\nabla \times \boldsymbol{A}) + \frac{1}{c^2}\frac{\partial^2}{\partial t^2}\underline{\underline{\varepsilon}}\boldsymbol{A} = 0. \tag{9}$$

The requirement of continuity of the tangential components of $\boldsymbol{E}$ following from equation (1) entails, in conjunction with equation (7), that at the interface between two constituents 1 and 2 with different electric permittivities, the tangential components of $\boldsymbol{A}$ must be continuous:

$$\boldsymbol{A}_{1t} = \boldsymbol{A}_{2t}. \tag{10}$$

Likewise, the requirement of continuity of the normal component of $\boldsymbol{D}$ following from equation (4) entails, in conjunction with equations (5) and (7), the relation for $\boldsymbol{A}$,

$$\nabla \cdot \left(\frac{\partial}{\partial t}\underline{\underline{\varepsilon}}\boldsymbol{A}\right) = 0, \tag{11}$$

which shows that at the interface between two constituents 1 and 2 with different electric permittivities, the normal component of $\underline{\underline{\varepsilon}}\boldsymbol{A}$ must be continuous:

$$\left(\underline{\underline{\varepsilon}}_1 \boldsymbol{A}_1\right)_n = \left(\underline{\underline{\varepsilon}}_2 \boldsymbol{A}_2\right)_n. \tag{12}$$

If, in the case of a harmonic time dependence with frequency ω, the vector potential $\boldsymbol{A}$ is assumed in the complex shape

$$\boldsymbol{A}(\boldsymbol{r}, t) = \tilde{\boldsymbol{A}}(\boldsymbol{r}) \exp(-\mathrm{i}\omega t) \tag{13}$$

with the space-dependent part $\tilde{\boldsymbol{A}}$, then equation (9) changes into the master equation for $\tilde{\boldsymbol{A}}$:

$$\Delta \tilde{\boldsymbol{A}} + k_0^2 \underline{\underline{\varepsilon}} \tilde{\boldsymbol{A}} = 0 \tag{14}$$

with the wavenumber of electromagnetic radiation propagating through a vacuum space, $k_0 = \omega/c$.

Studies of the optical properties of the composite draw on considerations of the flow of electromagnetic energy, $\boldsymbol{S}$, defined by

$$\boldsymbol{S} = \frac{c}{4\pi}(\boldsymbol{E} \times \boldsymbol{H}). \tag{15}$$

Making recourse to the representations of the electric field $\boldsymbol{E}$ and the magnetic field $\boldsymbol{H}$, equations (6) and (7), and assuming that the vector potential $\boldsymbol{A}$ herein, as a solution of equation (14) using equation (13), is of the plane-wave type

$$\boldsymbol{A}(\boldsymbol{r}, t) = \boldsymbol{a} \exp\left[\mathrm{i}\left(\boldsymbol{k}_\varepsilon \cdot \boldsymbol{r} - \omega t\right)\right] \tag{16}$$

with a complex amplitude $\boldsymbol{a}$ and a real wavevector $\boldsymbol{k}_\varepsilon$, the space- or time-averaged flow of electromagnetic energy, $\bar{\boldsymbol{S}}$, given by

$$\bar{\boldsymbol{S}} = \frac{1}{8\pi}\left[\left(\nabla \times \boldsymbol{A}^*\right) \times \frac{\partial \boldsymbol{A}}{\partial t}\right] \tag{17}$$

succinctly reads [29]

$$\bar{\boldsymbol{S}} = \frac{\omega}{8\pi}|\boldsymbol{a}|^2 \boldsymbol{k}_\varepsilon. \tag{18}$$

3. Theory of optical properties

Let us now consider a one-dimensional, layered photonic composite with periodically alternating dielectric constituents a and b of respective thicknesses d_a and d_b defining the primitive translation $d = d_a + d_b$ along the z-axis and occupying the half-space $z \geqslant 0$, covered by a superconducting surface layer s of thickness d_s extending within the range $-d_s \leqslant z < 0$, both in regard of a Cartesian coordinate system x, y, z. The dielectric constituents are supposed to be delineated by fixed values of the principal components of the respective tensors of electric permittivity $\varepsilon_\nu = \varepsilon_a > 1$ and $\varepsilon_\nu = \varepsilon_b > 1$, neglecting electromagnetic dissipation and assuming crystalline isotropy, whereas the superconducting layer is understood to be characterized by the principal components of the tensor of electric permittivity, $\varepsilon_\nu = \varepsilon_{s,\nu}$, derived in the appendix, taking into account electromagnetic dissipation and crystalline anisotropy, for $\nu = x, y$. We envisage that linearly polarized electromagnetic radiation in the form of TE polarized waves, labelled by $\nu = x$, or TM polarized waves, labelled by $\nu = y$, propagating in the positive z-direction through the vacuum space $z < -d_s$ is normally incident onto the surface $z = -d_s$ of the superconducting layer coating the dielectric photonic composite, as shown in figure 1. Investigations of the transmittance T_ν, reflectance R_ν and absorptance A_ν of such a composite, with $\nu = x, y$ probing either type of polarization, imply solving equation (14) for the space-dependent part of the vector potential separately in $z \geqslant 0$ and $-d_s \leqslant z < 0$ as well as $z < -d_s$ and joining the solutions together smoothly at $z = 0$ and $z = -d_s$; a procedure which, from equations (6) and (7), ensures continuity of the tangential components of both the electric and the magnetic field. Making recourse to equation (18) for the space- or time-averaged flow of electromagnetic energy then permits assessments of these optical properties straightforwardly.

3.1. Photonic modes and bands

We start by establishing the photonic modes of the dielectric composite in the half-space $z \geqslant 0$. Utilizing previous results [30], we have for $nd \leqslant z < nd + d_a$ with $n = 0, 1, 2, \ldots$

$$\begin{aligned}\tilde{A}_\nu(z) = {} & A_1 \exp\left[-\mathrm{i}\left(k_z + k_a\right) nd\right] \exp(\mathrm{i}k_a z) \\ & + A_2 \exp\left[-\mathrm{i}\left(k_z - k_a\right) nd\right] \exp\left(-\mathrm{i}k_a z\right)\end{aligned} \tag{19}$$

and for $nd + d_a \leqslant z < (n+1)d$ with $n = 0, 1, 2, \ldots$

$$\begin{aligned}\tilde{A}_\nu(z) = {} & B_1 \exp\left[-\mathrm{i}\left(k_z + k_b\right) nd\right] \exp\left(\mathrm{i}k_b z\right) \\ & + B_2 \exp\left[-\mathrm{i}\left(k_z - k_b\right) nd\right] \exp\left(-\mathrm{i}k_b z\right),\end{aligned} \tag{20}$$

upon introducing the wavenumber of these modes, k_z, apart from the wavenumbers $k_a = k_0 n_a$ and $k_b = k_0 n_b$ linked to the refractive indices of the dielectric constituents, $n_a = \varepsilon_a^{1/2}$ and $n_b = \varepsilon_b^{1/2}$; the amplitudes A_1, A_2 and B_1, B_2, determined up to an arbitrary non-zero factor, read

$$\begin{aligned}A_1 = {} & -\left(k_z - k_b\right)\left(k_a + k_b\right) \exp\left(\mathrm{i}k_b d_b\right) \\ & + \left(k_z + k_b\right)\left(k_a - k_b\right) \exp\left(-\mathrm{i}k_b d_b\right) \\ & + 2k_b\left(k_z - k_a\right) \exp\left[\mathrm{i}\left(k_z d - k_a d_a\right)\right]\end{aligned} \tag{21}$$

and

$$\begin{aligned}A_2 = {} & \left(k_z + k_b\right)\left(k_a + k_b\right) \exp\left(-\mathrm{i}k_b d_b\right) \\ & - \left(k_z - k_b\right)\left(k_a - k_b\right) \exp\left(\mathrm{i}k_b d_b\right) \\ & - 2k_b\left(k_z + k_a\right) \exp\left[\mathrm{i}\left(k_z d + k_a d_a\right)\right]\end{aligned} \tag{22}$$

as well as

$$\begin{aligned}B_1 = {} & \left(k_z + k_a\right)\left(k_a - k_b\right) \exp\left[-\mathrm{i}\left(k_b d - k_a d_a\right)\right] \\ & + \left(k_z - k_a\right)\left(k_a + k_b\right) \exp\left[-\mathrm{i}\left(k_b d + k_a d_a\right)\right] \\ & - 2k_a\left(k_z - k_b\right) \exp\left[-\mathrm{i}\left(k_z d + k_b d_a\right)\right]\end{aligned} \tag{23}$$

and

$$\begin{aligned}B_2 = {} & -\left(k_z + k_a\right)\left(k_a + k_b\right) \exp\left[\mathrm{i}\left(k_b d + k_a d_a\right)\right] \\ & - \left(k_z - k_a\right)\left(k_a - k_b\right) \exp\left[\mathrm{i}\left(k_b d - k_a d_a\right)\right] \\ & + 2k_a\left(k_z + k_b\right) \exp\left[-\mathrm{i}\left(k_z d - k_b d_a\right)\right].\end{aligned} \tag{24}$$

The dispersion of the photonic modes itself follows from the implicit equation

$$\begin{aligned}& \cos\left(k_a d_a\right) \cos\left(k_b d_b\right) - \frac{1}{2}\left(\frac{n_a}{n_b} + \frac{n_b}{n_a}\right) \sin\left(k_b d_b\right) \sin\left(k_a d_a\right) \\ & = \cos(k_z d),\end{aligned} \tag{25}$$

which defines the relation $\omega = \omega_j(k_z)$ for varying wavenumber k_z, the label $j = 0, 1, 2, \ldots$ numbering the photonic bands and gaps appropriate to the chosen direction of radiation incidence and types of polarization; it simultaneously implies the relation

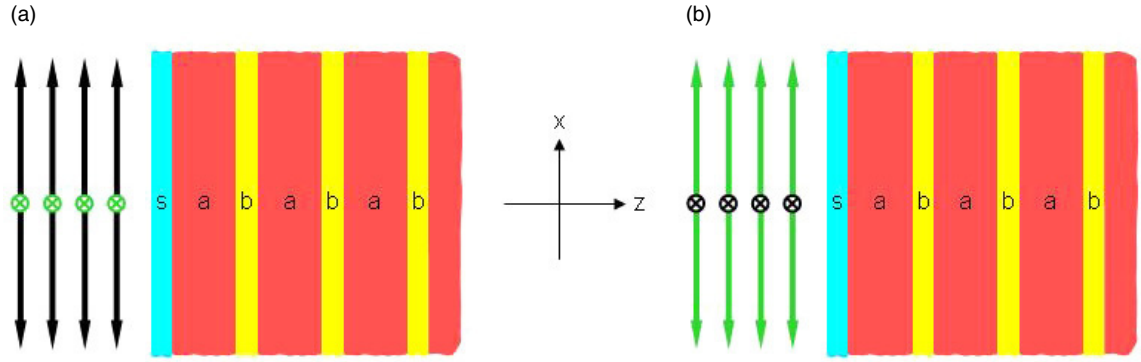

Figure 1. Schematic view of the layered photonic composite with dielectric constituents a and b covered by a superconducting surface layer s. The normally incident electromagnetic radiation is symbolized in the case of (a) TE polarization with the electric field (dark bold arrows) oriented parallel to the x-axis, the magnetic field (light crossed circles) oriented parallel to the y-axis and (b) TM polarization with the magnetic field (light bold arrows) oriented parallel to the x-axis, the electric field (dark crossed circles) oriented parallel to the y-axis of a Cartesian coordinate system x, y, z.

(This figure is in colour only in the electronic version)

$k_z = k_z(\omega_j)$ for varying frequency ω_j of the photonic bands and gaps with label $j = 0, 1, 2, \ldots$ called for in the evaluation of the optical properties examined below. We comment that for the propagating band modes, k_z is real and confined to the first Brillouin zone $-\pi/d \leqslant k_z \leqslant \pi/d$, whereas for the evanescent band-gap modes, k_z is complex and given by $k_z = G_z/2 - \mathrm{i}q$, with the reciprocal lattice translation $G_z = 0$ or $\pm 2\pi/d$ applying to the gaps adjoining air or, respectively, dielectric bands, and the imaginary part $q > 0$.

The photonic modes within the range of the superconducting layer $-d_s \leqslant z < 0$ are

$$\tilde{A}_\nu(z) = P_\nu \exp(\mathrm{i}k_{s,\nu}z) + Q_\nu \exp\left(-\mathrm{i}k_{s,\nu}z\right), \qquad (26)$$

upon introducing the wavevector components $k_{s,\nu} = k_0 n_{s,\nu}$ linked to the principal components of the tensor of refractive index of the superconducting layer, $n_{s,\nu} = \varepsilon_{s,\nu}^{1/2}$, and using the abbreviations

$$P_\nu = \frac{1}{2}\left[\left(1 + \frac{n_a}{n_{s,\nu}}\right)A_1 + \left(1 - \frac{n_a}{n_{s,\nu}}\right)A_2\right] \qquad (27)$$

and

$$Q_\nu = \frac{1}{2}\left[\left(1 - \frac{n_a}{n_{s,\nu}}\right)A_1 + \left(1 + \frac{n_a}{n_{s,\nu}}\right)A_2\right]; \qquad (28)$$

in the vacuum space $z < -d_s$ they read

$$\tilde{A}_\nu(z) = V_{1,\nu}\exp(\mathrm{i}k_0 z) + V_{2,\nu}\exp(-\mathrm{i}k_0 z), \qquad (29)$$

with amplitudes $V_{1,\nu}$, $V_{2,\nu}$ given by

$$V_{1,\nu} = \tfrac{1}{2}[(1 + n_{s,\nu})P_\nu \exp(-\mathrm{i}k_{s,\nu}d_s) + (1 - n_{s,\nu})Q_\nu \exp(\mathrm{i}k_{s,\nu}d_s)]\exp(\mathrm{i}k_0 d_s) \qquad (30)$$

and

$$V_{2,\nu} = \tfrac{1}{2}[(1 - n_{s,\nu})P_\nu \exp(-\mathrm{i}k_{s,\nu}d_s) + (1 + n_{s,\nu})Q_\nu \exp(\mathrm{i}k_{s,\nu}d_s)]\exp(-\mathrm{i}k_0 d_s). \qquad (31)$$

3.2. Transmittance, reflectance and absorptance

We now examine the optical properties of the coated dielectric composite for the chosen direction of radiation incidence and types of polarization. From equation (18) together with equation (19), the space- or time-averaged net flow of electromagnetic energy of the transmitted waves is

$$\bar{S}_{z,12} = \pm\frac{\omega}{8\pi}\left[|A_1|^2 - |A_2|^2\right]k_a, \qquad (32)$$

referring to the amplitudes A_1, A_2 given by equations (21) and (22); conversely, from equation (18) together with equation (29), the space- or time-averaged flows of electromagnetic energy of the incident and reflected waves are

$$\bar{S}_{z,1,\nu} = \frac{\omega}{8\pi}\left|V_{1,\nu}\right|^2 k_0, \qquad \bar{S}_{z,2,\nu} = -\frac{\omega}{8\pi}\left|V_{2,\nu}\right|^2 k_0, \qquad (33)$$

resorting to the amplitudes $V_{1,\nu}$, $V_{2,\nu}$ given by equations (30) and (31).

Using equations (32) and (33), the transmittance T_ν defined, in the case of dielectric bands for $-\pi/d \leqslant k_z < 0$ and adjoining gaps or, respectively, air bands for $0 \leqslant k_z \leqslant \pi/d$ and adjoining gaps, with $l = 0, 1, 2, \ldots$, according to

$$\left.\begin{matrix} T_{2l,\nu}^{(-)} \\ T_{2l+1,\nu}^{(+)} \end{matrix}\right\} = \left|\frac{\bar{S}_{z,12}}{\bar{S}_{z,1,\nu}}\right| \qquad (34)$$

thus reads

$$\left.\begin{matrix} T_{2l,\nu}^{(-)} \\ T_{2l+1,\nu}^{(+)} \end{matrix}\right\} = 4n_a \times \frac{|A_1|^2 - |A_2|^2}{|(1 + n_{s,\nu})P_\nu \exp(-\mathrm{i}k_{s,\nu}d_s) + (1 - n_{s,\nu})Q_\nu \exp(\mathrm{i}k_{s,\nu}d_s)|^2}; \qquad (35)$$

likewise, this quantity defined, in the case of dielectric bands for $0 \leqslant k_z \leqslant \pi/d$ and adjoining gaps or, respectively, air bands

for $-\pi/d \leqslant k_z < 0$ and adjoining gaps, with $l = 0, 1, 2, \ldots$, according to

$$\left.\begin{matrix} T^{(+)}_{2l,\nu} \\ T^{(-)}_{2l+1,\nu} \end{matrix}\right\} = \left|\frac{\bar{S}_{z,12}}{\bar{S}_{z,2,\nu}}\right| \tag{36}$$

reads

$$\left.\begin{matrix} T^{(+)}_{2l,\nu} \\ T^{(-)}_{2l+1,\nu} \end{matrix}\right\} = 4n_a \times \frac{|A_2|^2 - |A_1|^2}{|(1-n_{s,\nu})P_\nu \exp(-\mathrm{i}k_{s,\nu}d_s) + (1+n_{s,\nu})Q_\nu \exp(\mathrm{i}k_{s,\nu}d_s)|^2}. \tag{37}$$

Both of these cases make use of the abbreviations P_ν and Q_ν spelt out in equations (27), (28) and require exploiting equation (25). We note the limits of the bare dielectric composite

$$\lim_{d_s\to 0}\left\{\begin{matrix} T^{(-)}_{2l,\nu} \\ T^{(+)}_{2l+1,\nu} \end{matrix}\right\} = 4n_a \frac{|A_1|^2 - |A_2|^2}{|(1+n_a)\,A_1 + (1-n_a)\,A_2|^2} \tag{38}$$

and

$$\lim_{d_s\to 0}\left\{\begin{matrix} T^{(+)}_{2l,\nu} \\ T^{(-)}_{2l+1,\nu} \end{matrix}\right\} = 4n_a \frac{|A_2|^2 - |A_1|^2}{|(1-n_a)\,A_1 + (1+n_a)\,A_2|^2}. \tag{39}$$

Furthermore, the limits of the bare dielectric composite degenerating into a semi-infinite, homogeneous dielectric

$$\lim_{\varepsilon_b\to\varepsilon_a}\lim_{d_s\to 0}\left\{\begin{matrix} T^{(-)}_{2l,\nu} \\ T^{(+)}_{2l+1,\nu} \end{matrix}\right\} = \lim_{\varepsilon_b\to\varepsilon_a}\lim_{d_s\to 0}\left\{\begin{matrix} T^{(+)}_{2l,\nu} \\ T^{(-)}_{2l+1,\nu} \end{matrix}\right\} = \frac{4n_a}{(1+n_a)^2} \tag{40}$$

apply too, as they should.

Using equation (33), the reflectance R_ν defined, in the case of dielectric bands for $-\pi/d \leqslant k_z < 0$ and adjoining gaps or, respectively, air bands for $0 \leqslant k_z \leqslant \pi/d$ and adjoining gaps, with $l = 0, 1, 2, \ldots$, according to

$$\left.\begin{matrix} R^{(-)}_{2l,\nu} \\ R^{(+)}_{2l+1,\nu} \end{matrix}\right\} = \left|\frac{\bar{S}_{z,2,\nu}}{\bar{S}_{z,1,\nu}}\right| \tag{41}$$

thus reads

$$\left.\begin{matrix} R^{(-)}_{2l,\nu} \\ R^{(+)}_{2l+1,\nu} \end{matrix}\right\} = \left|\frac{(1-n_{s,\nu})P_\nu \exp(-\mathrm{i}k_{s,\nu}d_s) + (1+n_{s,\nu})Q_\nu \exp(\mathrm{i}k_{s,\nu}d_s)}{(1+n_{s,\nu})P_\nu \exp(-\mathrm{i}k_{s,\nu}d_s) + (1-n_{s,\nu})Q_\nu \exp(\mathrm{i}k_{s,\nu}d_s)}\right|^2; \tag{42}$$

similarly, this quantity defined, in the case of dielectric bands for $0 \leqslant k_z \leqslant \pi/d$ and adjoining gaps or, respectively, air bands for $-\pi/d \leqslant k_z < 0$ and adjoining gaps, with $l = 0, 1, 2, \ldots$, according to

$$\left.\begin{matrix} R^{(+)}_{2l,\nu} \\ R^{(-)}_{2l+1,\nu} \end{matrix}\right\} = \left|\frac{\bar{S}_{z,1,\nu}}{\bar{S}_{z,2,\nu}}\right| \tag{43}$$

reads

$$\left.\begin{matrix} R^{(+)}_{2l,\nu} \\ R^{(-)}_{2l+1,\nu} \end{matrix}\right\} = \left|\frac{(1+n_{s,\nu})P_\nu \exp(-\mathrm{i}k_{s,\nu}d_s) + (1-n_{s,\nu})Q_\nu \exp(\mathrm{i}k_{s,\nu}d_s)}{(1-n_{s,\nu})P_\nu \exp(-\mathrm{i}k_{s,\nu}d_s) + (1+n_{s,\nu})Q_\nu \exp(\mathrm{i}k_{s,\nu}d_s)}\right|^2. \tag{44}$$

Again, both of these cases make use of the abbreviations P_ν and Q_ν spelt out in equations (27), (28) and require exploiting equation (25). We note the limits of the bare dielectric composite

$$\lim_{d_s\to 0}\left\{\begin{matrix} R^{(-)}_{2l,\nu} \\ R^{(+)}_{2l+1,\nu} \end{matrix}\right\} = \left|\frac{(1-n_a)\,A_1 + (1+n_a)\,A_2}{(1+n_a)\,A_1 + (1-n_a)\,A_2}\right|^2 \tag{45}$$

and

$$\lim_{d_s\to 0}\left\{\begin{matrix} R^{(+)}_{2l,\nu} \\ R^{(-)}_{2l+1,\nu} \end{matrix}\right\} = \left|\frac{(1+n_a)\,A_1 + (1-n_a)\,A_2}{(1-n_a)\,A_1 + (1+n_a)\,A_2}\right|^2. \tag{46}$$

Furthermore, the limits of the bare dielectric composite degenerating into a semi-infinite, homogeneous dielectric

$$\lim_{\varepsilon_b\to\varepsilon_a}\lim_{d_s\to 0}\left\{\begin{matrix} R^{(-)}_{2l,\nu} \\ R^{(+)}_{2l+1,\nu} \end{matrix}\right\} = \lim_{\varepsilon_b\to\varepsilon_a}\lim_{d_s\to 0}\left\{\begin{matrix} R^{(+)}_{2l,\nu} \\ R^{(-)}_{2l+1,\nu} \end{matrix}\right\} = \left(\frac{1-n_a}{1+n_a}\right)^2 \tag{47}$$

apply too, as they should.

Finally, from equations (35), (37) and (42), (44), the absorptance A_ν is defined such that the conservation relations with $j = 0, 1, 2, \ldots$

$$T^{(-)}_{j,\nu} + R^{(-)}_{j,\nu} + A^{(-)}_{j,\nu} = T^{(+)}_{j,\nu} + R^{(+)}_{j,\nu} + A^{(+)}_{j,\nu} = 1 \tag{48}$$

hold, in keeping with the need for continuity of the flow of electromagnetic energy.

4. Numerical results

To appraise the effect of a superconducting surface layer on the optical properties of the layered photonic composite, we propose that the dielectric constituents are made from almost cubic perovskites, whose electric permittivity can be widely tuned by proper doping and which allow nearly perfect epitaxial growth. Furthermore, we imagine that the superconducting layer consists of a single-crystalline, highly anisotropic and very pure yttrium–barium cuprate epitaxially grown on the composite substrate such that its (electrically 'light') crystallographic a-axis and its (electrically 'heavy') crystallographic c-axis coincide, respectively, with the x- and y-axes of the chosen Cartesian coordinate system x, y, z. Our numerical evaluations, shown graphically below, relate to the geometrical and materials data listed in table 1.

Figure 2 illustrates the dispersion of the photonic modes of the bare dielectric composite derived from equation (25) and figure 3 depicts the variation with frequency of the pertinent transmittance T_ν and reflectance R_ν in the range spanned by

Table 1. Geometrical and materials data used in calculations.

Data relating to the dielectric photonic composite:	
Primitive translation, d (m)	5.0×10^{-6}
Relative layer thickness, d_a/d	0.75
Electric permittivity, ε_a	20
Relative layer thickness, d_b/d	0.25
Electric permittivity, ε_b	5
Data relating to the superconducting surface layer:	
Critical temperature, T_c (K)	90 [31]
Half-gap energy at absolute zero, Δ_0 (eV)	3.0×10^{-2} [31]
London tensor x-component at absolute zero, $\Lambda_{s,x}^{(0)}$ (s^2)	2.1×10^{-30} [32, 33]
London tensor y-component at absolute zero, $\Lambda_{s,y}^{(0)}$ (s^2)	1.9×10^{-28} [32, 33]
Scattering rate constant, α (s^{-1})	1.4×10^{13} [34]

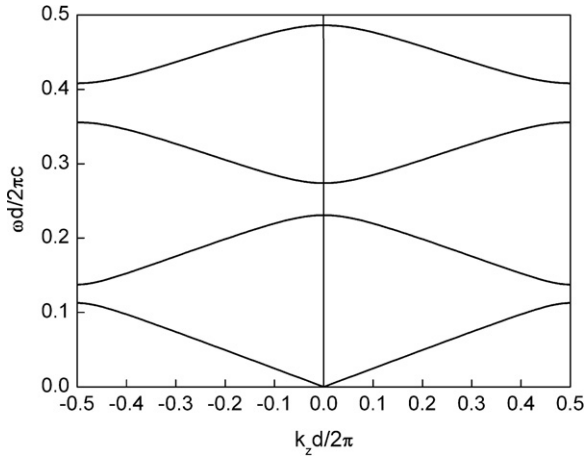

Figure 2. Dispersion of the photonic modes of the bare dielectric composite in the cases of TE polarization, where $\nu = x$, and TM polarization, where $\nu = y$, due to on-axis propagation: normalized frequency $\omega d/2\pi c$ of the lowest four photonic bands as a function of the normalized wavenumber $k_z d/2\pi$ within the first Brillouin zone.

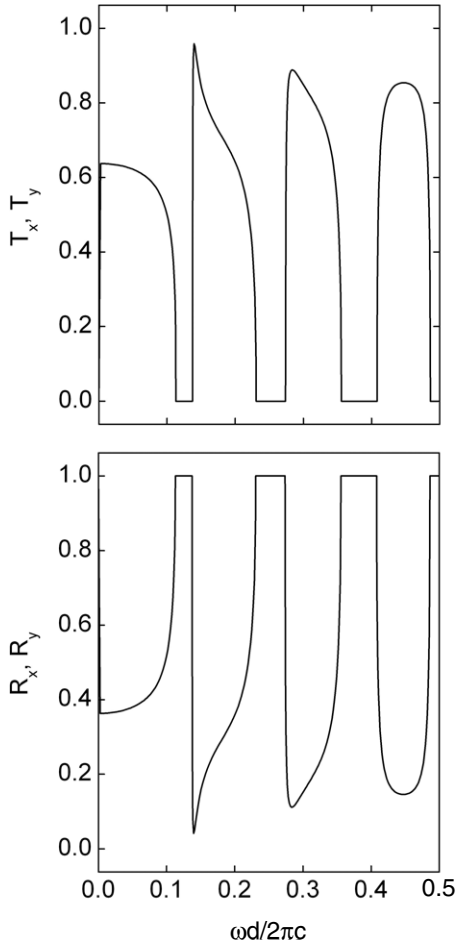

Figure 3. Transmittance T_ν and reflectance R_ν of the bare dielectric composite as a function of the normalized frequency $\omega d/2\pi c$ in the cases of TE polarization, where $\nu = x$, and TM polarization, where $\nu = y$, due to on-axis propagation.

the lowest four photonic bands, as calculated from the limiting equations (38), (39) and (45), (46), assuming TE polarization, where $\nu = x$, and TM polarization, where $\nu = y$, for normally incident electromagnetic radiation. We remark that, since in accord with our premise about the dielectric constituents, no electromagnetic dissipation takes place therein, T_ν and R_ν are strictly complementary regarding each type of polarization at any given frequency, obviously bearing witness to the sequence of photonic bands and gaps.

Figures 4–9 present the variation with frequency of the transmittance T_ν, reflectance R_ν and absorptance A_ν of the coated dielectric composite obtained from equations (35), (37), (42), (44) and (48), in the cases of TE polarization, where $\nu = x$, and TM polarization, where $\nu = y$, for on-axis propagation, examining two normalized thicknesses of the superconducting layer, $d_s/d = 0.025$ and $d_s/d = 0.25$, and three representative temperatures, the helium temperature $T = 4.2$ K, the nitrogen temperature $T = 77$ K and the critical temperature $T_c = 90$ K. Dwelling on the physical data chosen to characterize the dielectric composite, the range of frequency discussed here (with its maximum centred in the infrared part of the spectrum of electromagnetic radiation) encompasses the pair breaking frequency of the superconducting constituent at all temperatures; the respective plasma frequencies, however, lie outside this range for either type of polarization.

A comparison of the optical properties of the coated dielectric composite with those of the corresponding bare composite reveals obvious similarities, but even more substantial differences depending on the thickness of the superconducting layer, frequency, temperature and polarization of the incident electromagnetic radiation. Thus, since only

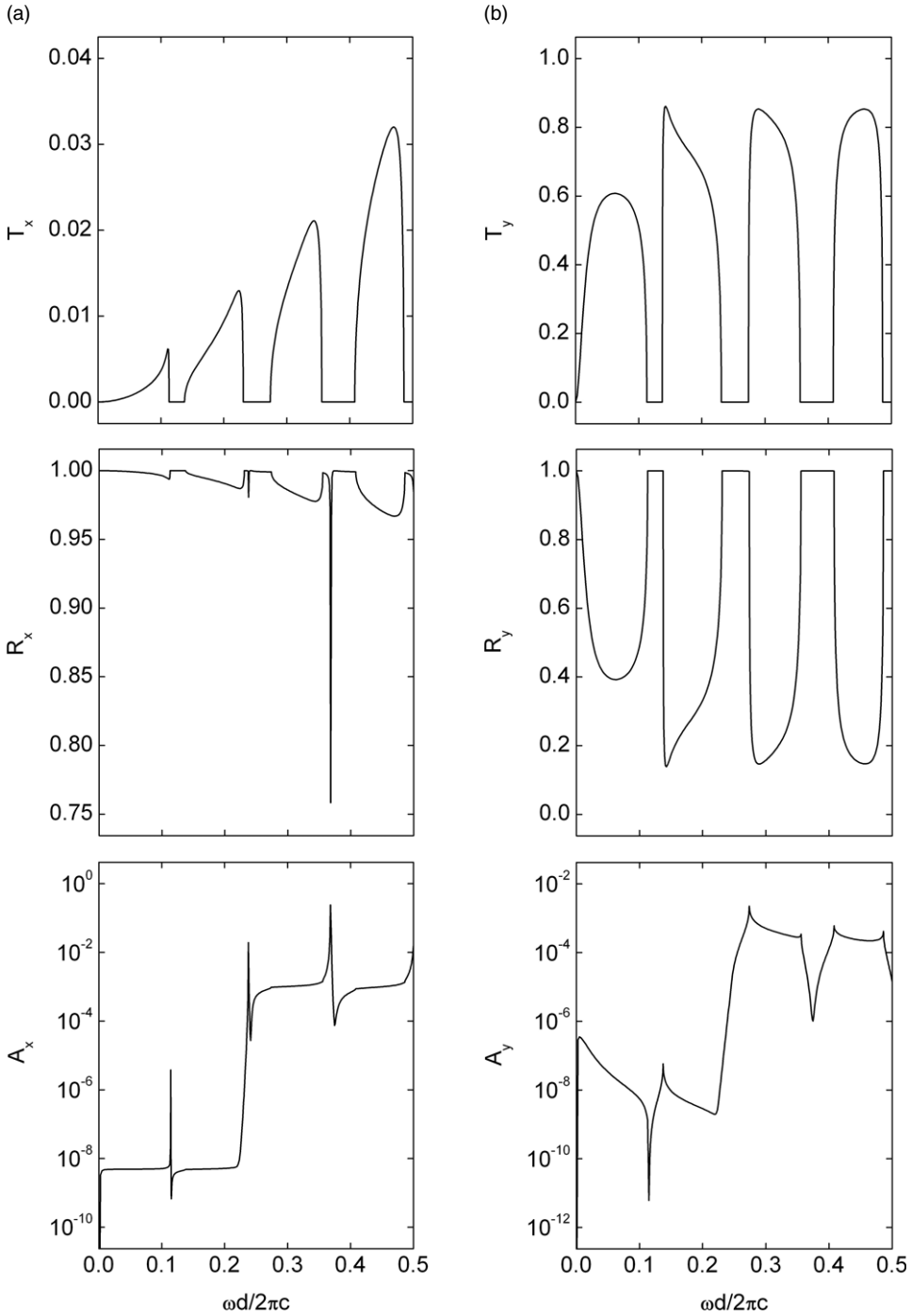

Figure 4. Transmittance T_ν, reflectance R_ν and absorptance A_ν of the coated dielectric composite as a function of the normalized frequency $\omega d/2\pi c$ for a superconducting surface layer of normalized thickness $d_s/d = 0.025$ at the helium temperature $T = 4.2$ K in the case of (a) TE polarization, addressing the component of the normalized London penetration depth $\lambda_{s,\nu}/d_s = 0.980$, where $\nu = x$, and (b) TM polarization, addressing the component of the normalized London penetration depth $\lambda_{s,\nu}/d_s = 9.326$, where $\nu = y$, due to on-axis propagation. The normalized pair breaking frequency here is $\omega_s d/2\pi c = 0.242$.

the band modes propagate, finite transmittances, exposed in the upper plots of figures 4–9, solely appear across the photonic bands, with zero transmittance due to the evanescent modes over the photonic gaps, just as in the upper plot of figure 3. However, for the thinner superconducting layer (figures 4–6), there is a monotonic increase of the maxima of the transmittance T_x with the number of the bands and a depression of the transmittance by one or two orders of magnitude, depending on frequency, in the case of TE polarization, whereas the variation with frequency of the transmittance T_y in the case of TM polarization is very much like for the bare composite at all temperatures considered here. By contrast, for the thicker superconducting layer (figures 7–9), there is a monotonic increase of the maxima

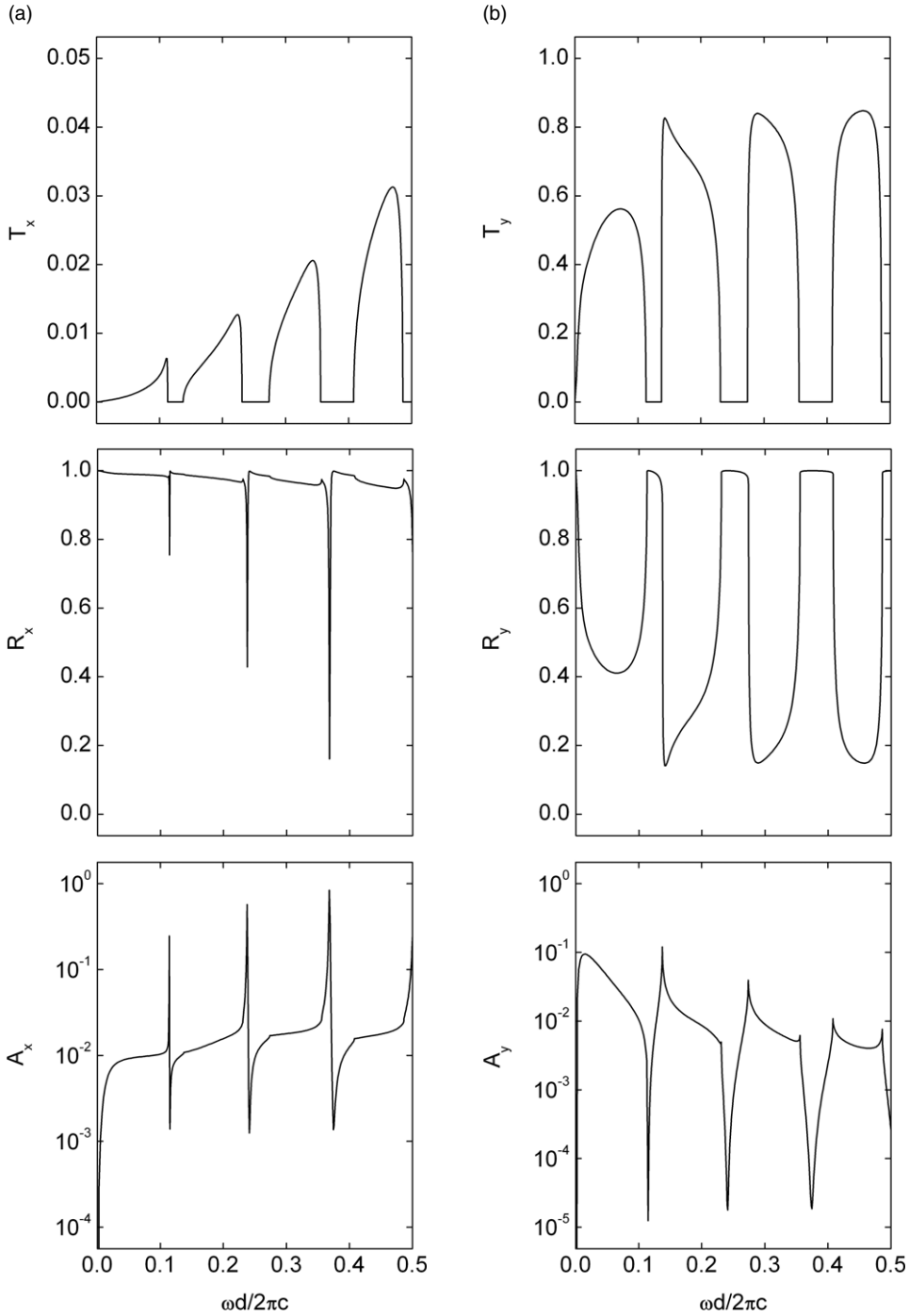

Figure 5. Transmittance T_ν, reflectance R_ν and absorptance A_ν of the coated dielectric composite as a function of the normalized frequency $\omega d/2\pi c$ for a superconducting surface layer of normalized thickness $d_s/d = 0.025$ at the nitrogen temperature $T = 77$ K in the case of (a) TE polarization, addressing the component of the normalized London penetration depth $\lambda_{s,\nu}/d_s = 1.439$, where $\nu = x$, and (b) TM polarization, addressing the component of the normalized London penetration depth $\lambda_{s,\nu}/d_s = 13.687$, where $\nu = y$, due to on-axis propagation. The normalized pair breaking frequency here is $\omega_s d/2\pi c = 0.189$.

of the transmittance T_y with the number of the bands in the case of TM polarization at all temperatures considered here, whilst the transmittance T_x is depressed by 5–10 orders of magnitude, depending on both frequency and temperature, in the case of TE polarization. Taken together, these facets yield a maximum optical selectivity $(T_y/T_x)_{\max}$ of the order of 10^2 for the thinner superconducting layer and of the order of 10^9 for the thicker superconducting layer in switching from TE to TM polarization, with a moderate dependence on temperature for either of the thicknesses addressed.

Since at frequencies within the gaps between the photonic bands, electromagnetic radiation cannot be transmitted, nevertheless absorbed, the reference to photonic bands and gaps as regards the reflectances shown in the central plots

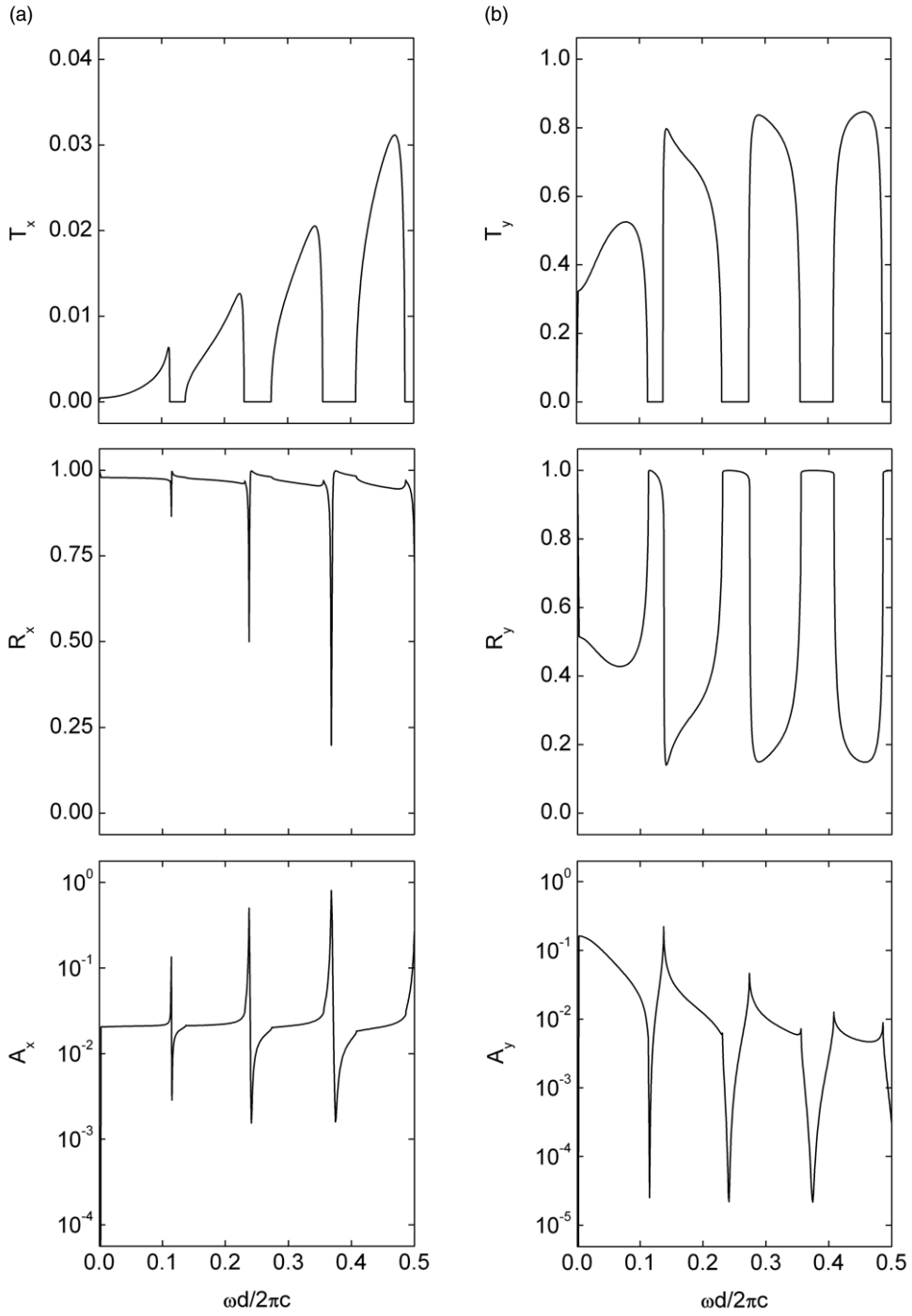

Figure 6. Transmittance T_ν, reflectance R_ν and absorptance A_ν of the coated dielectric composite as a function of the normalized frequency $\omega d/2\pi c$ for a superconducting surface layer of normalized thickness $d_s/d = 0.025$ at the critical temperature $T_c = 90$ K in the case of (a) TE polarization, addressing the component of the normalized London penetration depth $\lambda_{s,\nu}/d_s = \infty$, where $\nu = x$, and (b) TM polarization, addressing the component of the normalized London penetration depth $\lambda_{s,\nu}/d_s = \infty$, where $\nu = y$, due to on-axis propagation. The normalized pair breaking frequency here is $\omega_s d/2\pi c = 0$.

of figures 4–9 is more involved (if at all extant) than that evident in the lower plot of figure 3. Thus, for the thinner superconducting layer (figures 4–6), the reflectance R_x is almost unity throughout, yet exhibits sharp dips at frequencies near the lower edges of the gaps, their depth increasing monotonically with the number of the gaps, in the case of TE polarization, whereas the variation with frequency of the reflectance R_y in the case of TM polarization is very much like for the bare composite, at all temperatures addressed. By contrast, for the thicker superconducting layer (figures 7–9), the reflectance R_y shows minima at frequencies within the photonic bands, their depth increasing monotonically with the number of the bands, in the case of TM polarization, unlike for the bare composite, at all temperatures addressed. The

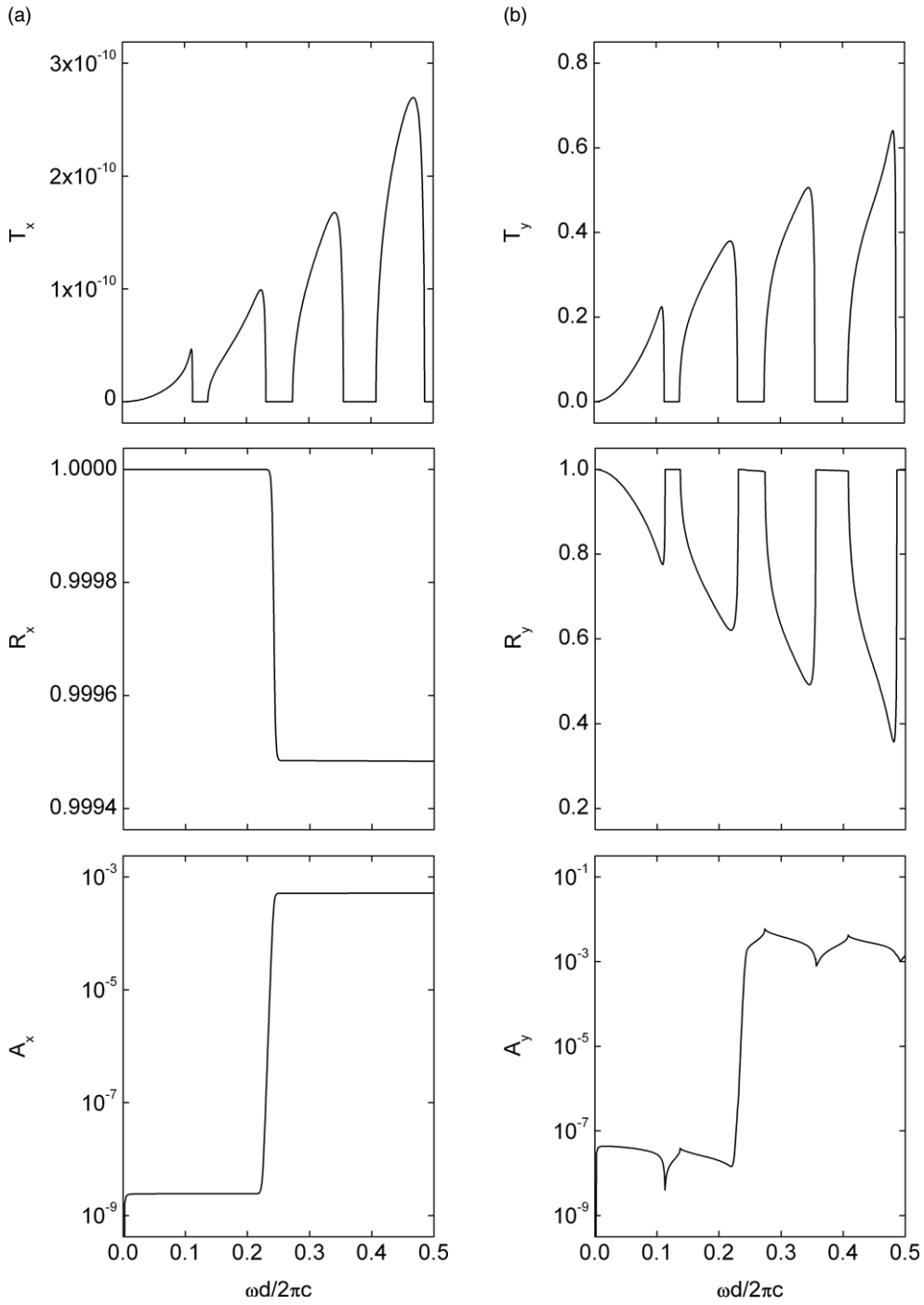

Figure 7. Transmittance T_ν, reflectance R_ν and absorptance A_ν of the coated dielectric composite as a function of the normalized frequency $\omega d/2\pi c$ for a superconducting surface layer of normalized thickness $d_s/d = 0.25$ at the helium temperature $T = 4.2$ K in the case of (a) TE polarization, addressing the component of the normalized London penetration depth $\lambda_{s,\nu}/d_s = 0.098$, where $\nu = x$, and (b) TM polarization, addressing the component of the normalized London penetration depth $\lambda_{s,\nu}/d_s = 0.933$, where $\nu = y$, due to on-axis propagation. The normalized pair breaking frequency here is $\omega_s d/2\pi c = 0.242$.

reflectance R_x in the case of TE polarization is again almost unity throughout, but reveals a minute step-like drop around the pair breaking frequency of the superconducting constituent at the temperature $T = 4.2$ K, a slightly more pronounced, smeared-out fall at the temperature $T = 77$ K and a rapid, monotonic decay at the temperature $T_c = 90$ K, without any sign of reference to the photonic bands and gaps.

The absorptances, originating from electromagnetic dissipation in the superconducting constituent, are displayed in the lower plots of figures 4–9. Accordingly, the following general characteristics appear to hold: electromagnetic dissipation builds up with temperature, as does the density of the normal electrons, irrespective of the thickness of the superconducting layer and type of polarization. Yet, for a fixed

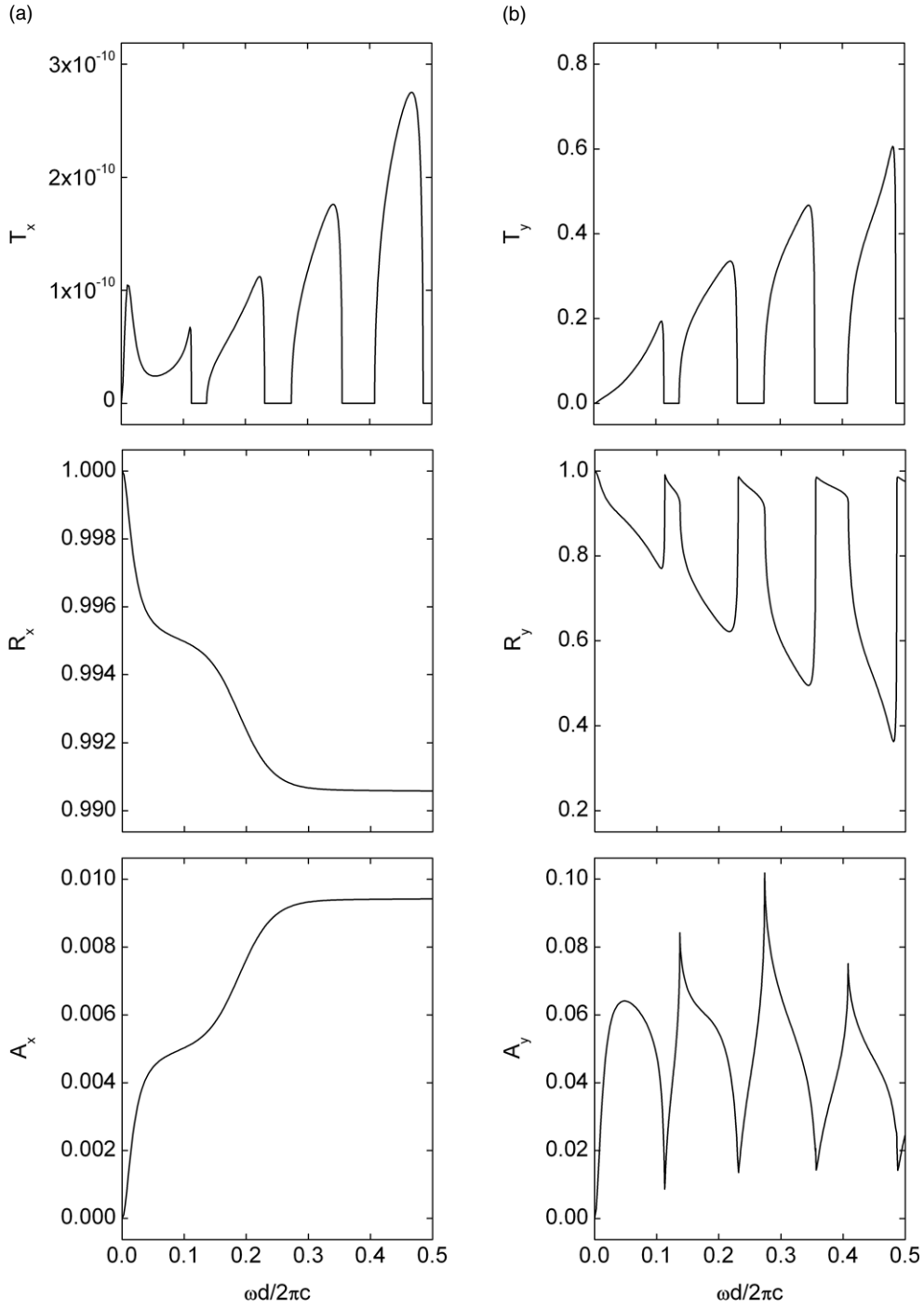

Figure 8. Transmittance T_ν, reflectance R_ν and absorptance A_ν of the coated dielectric composite as a function of the normalized frequency $\omega d/2\pi c$ for a superconducting surface layer of normalized thickness $d_s/d = 0.25$ at the nitrogen temperature $T = 77$ K in the case of (a) TE polarization, addressing the component of the normalized London penetration depth $\lambda_{s,\nu}/d_s = 0.144$, where $\nu = x$, and (b) TM polarization, addressing the component of the normalized London penetration depth $\lambda_{s,\nu}/d_s = 1.369$, where $\nu = y$, due to on-axis propagation. The normalized pair breaking frequency here is $\omega_s d/2\pi c = 0.189$.

thickness of this layer and a given frequency and temperature, it is stronger in the case of TE polarization than in the case of TM polarization owing to the higher normal conductivity, and hence the higher normal current density, along the x-direction as opposed to the y-direction; a trait particularly discernible at the lowest temperature addressed. Evidence of the underlying photonic band structure is more distinct for the thinner superconducting layer and TM polarization than for the thicker superconducting layer and TE polarization due to the stronger overall shielding effect prevailing in the latter case. Specifically, for the thinner superconducting layer (figures 4–6), the absorptance A_x manifests sharp spikes at frequencies near the lower edges of the photonic gaps, their height increasing monotonically with the number of the gaps, in the

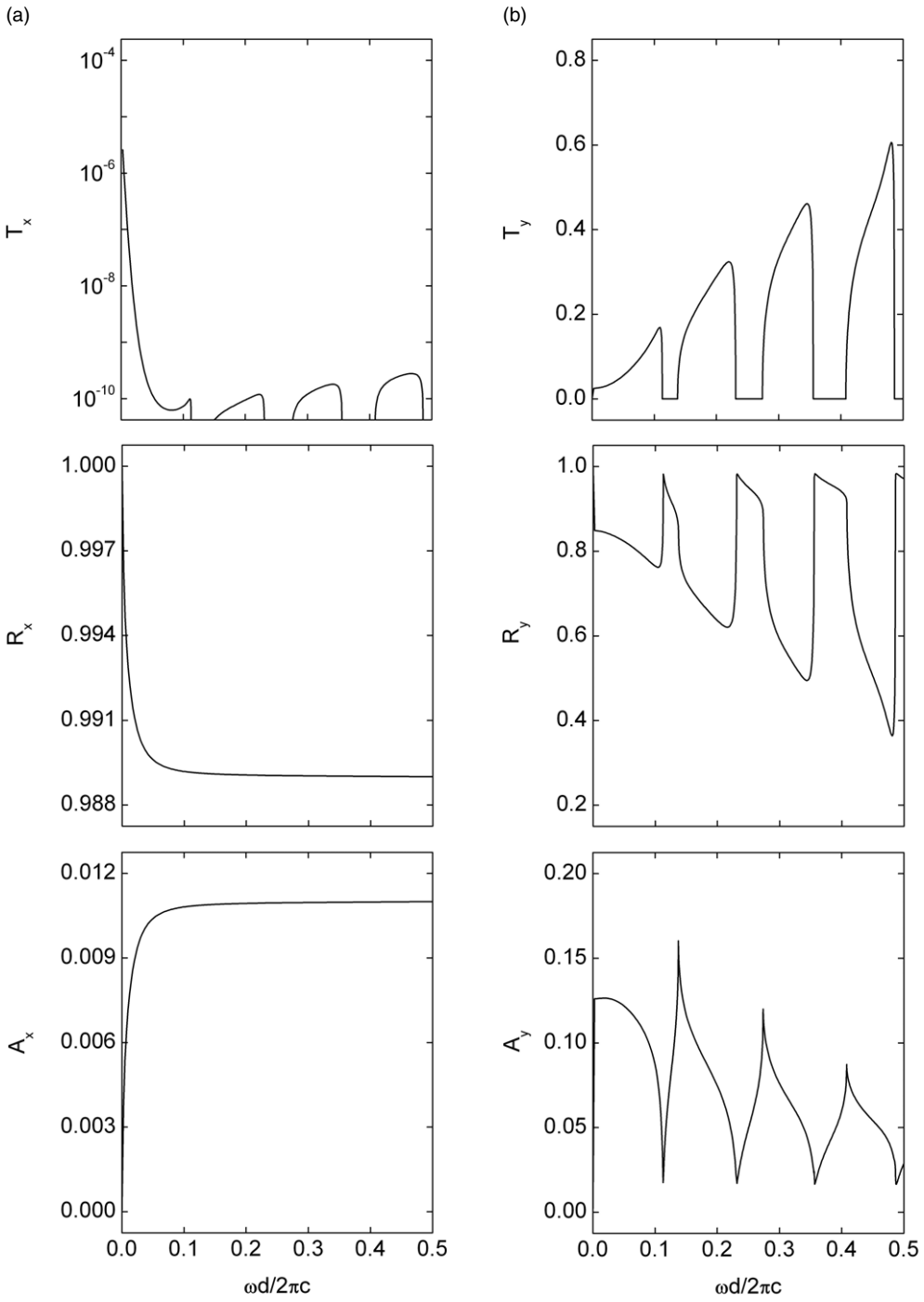

Figure 9. Transmittance T_ν, reflectance R_ν and absorptance A_ν of the coated dielectric composite as a function of the normalized frequency $\omega d/2\pi c$ for a superconducting surface layer of normalized thickness $d_s/d = 0.25$ at the critical temperature $T_c = 90$ K in the case of (a) TE polarization, addressing the component of the normalized London penetration depth $\lambda_{s,\nu}/d_s = \infty$, where $\nu = x$, and (b) TM polarization, addressing the component of the normalized London penetration depth $\lambda_{s,\nu}/d_s = \infty$, where $\nu = y$, due to on-axis propagation. The normalized pair breaking frequency here is $\omega_s d/2\pi c = 0$.

case of TE polarization at all temperatures considered here, but reveals a sudden increase around the pair breaking frequency of the superconducting constituent at the temperature $T = 4.2$ K, whereas the absorptance A_y displays minima at frequencies near the lower edges of the photonic gaps, their depth increasing monotonically with the number of the gaps, in the case of TM polarization at all temperatures addressed, yet shows a sudden rise around the pair breaking frequency of the superconducting constituent instead of a minimum at the above temperature. Similarly, for the thicker superconducting layer (figures 7–9), the variation with frequency of the absorptance A_y in the case of TM polarization is very much like for the thinner superconducting layer, although with its magnitude increased, at all temperatures addressed. By contrast, the

absorptance A_x in the case of TE polarization shows a step-like rise around the pair breaking frequency of the superconducting constituent at the temperature $T = 4.2$ K, a smeared-out ascent at the temperature $T = 77$ K and a steep, monotonic rise at the temperature $T_c = 90$ K, again without any trace of reference to the photonic bands and gaps; behaviour virtually complementary to that of the reflectance R_x at any given frequency, demonstrating a property of the superconductor alone.

We comment that, in reality, at frequencies far below the pair breaking frequency of the superconducting constituent at the temperature $T = 77$ K, the absorptance A_x in the case of TE polarization and the absorptance A_y in the case of TM polarization are expected to be somewhat enhanced compared with the predictions of figures 5 and 8 due to a coherence effect not embodied in the model taken as a basis for the respective tensor of electric permittivity. (For details see the appendix.) On the other hand, at the temperatures $T = 4.2$ K and $T_c = 90$ K, the absorptance A_x in the case of TE polarization and the absorptance A_y in the case of TM polarization are certainly reliably predicted by the figures 4, 6 and 7, 9 throughout the range of frequencies displayed.

5. Conclusions

In the framework of a vector potential approach, we have investigated, both analytically and numerically, the effect of a strongly anisotropic superconducting surface layer on the transmittance, reflectance and absorptance of a one-dimensional, layered dielectric composite with periodically alternating, isotropic constituents assuming linearly polarized, normally incident electromagnetic radiation. The underlying model of the electric permittivity of the superconducting constituent accounts for photonic excitation at frequencies both below and above the superconductor pair breaking frequency as well as thermal and normal scattering right up to the superconductor critical temperature. Resorting to an analysis of the propagating band modes and the evanescent band-gap modes, the transmittance, reflectance and absorptance of the coated composite have been established for two different thicknesses of the superconducting layer at three representative temperatures and compared with the corresponding quantities of the bare composite, in the cases of TE and TM polarization of the electromagnetic radiation. The optical properties addressed combine traits characteristic of the periodic dielectric composite and the superconducting layer too, revealing, e.g., band-like patterns of the transmittance and reflectance, but also step-like or smeared-out patterns of the reflectance and absorptance, depending on the thickness of the superconducting layer and temperature. By virtue of the anisotropy of the superconducting layer covering the dielectric composite, a marked reference of these features to the particular type of polarization persists. Thus, in switching from TE to TM polarization, the maximum optical selectivity can become gigantic, given an appropriate thickness of the superconducting layer, with a moderate dependence on temperature. This fact offers unique possibilities regarding practical applications of such a novel photonic composite as an efficient polarization filter for electromagnetic radiation tunable via the thickness of the covering layer and temperature.

Acknowledgment

Stimulating discussions with L Alff and I L Lyubchanskii are gratefully acknowledged.

Appendix. Tensor of electric permittivity of a superconductor

We introduce a working model of the tensor of electric permittivity of a superconductor which accounts for crystalline anisotropy, photonic excitation at arbitrary frequencies $\omega \geqslant 0$ as well as thermal excitation and normal scattering over the whole range of absolute temperature $0 \leqslant T \leqslant T_c$; features duly extending those of the allied representation of a generalized two-fluid model set forth before [35]. Resting upon a phenomenological approach, our model unites two key aspects of superconductivity, viz. the presence of both superelectrons ('Cooper pairs') and normal electrons in the superconducting state and the phase transition to the normal state caused by the incident electromagnetic radiation at temperatures below T_c.

Consider a bulk, single-crystalline superconductor of orthorhombic structure, with its principal crystallographic directions oriented parallel to the axes of the Cartesian coordinate system x, y, z, so that all (symmetric) second-rank tensors characterizing superconductor properties are entirely determined by their respective diagonal elements alone. Thus, a harmonic time dependence like in equation (13) yields for the principal components of the tensor of electric permittivity of the superconductor, $\varepsilon_{s,\nu}(\omega, T)$, with $\nu = x, y, z$,

$$\varepsilon_{s,\nu}(\omega, T) = 1 + \frac{4\pi \mathrm{i}}{\omega}\sigma_{s,\nu}(\omega, T). \tag{A.1}$$

The relevant components of the pertaining tensor of dynamic electrical conductivity, $\sigma_{s,\nu}(\omega, T)$, herein may be expressed as

$$\sigma_{s,\nu}(\omega, T) = f_<(\omega, T)\,\sigma_{s,\nu}^{(<)}(\omega, T) + f_>(\omega, T)\sigma_{s,\nu}^{(>)}(\omega, T), \tag{A.2}$$

where

$$f_<(\omega, T) = \frac{1}{\exp\left[\frac{\hbar(\omega-\omega_s(T))}{k_B T}\right] + 1} \tag{A.3}$$

denotes the probability for superelectrons coexisting alongside normal electrons due to thermal excitation and

$$f_>(\omega, T) = \frac{1}{\exp\left[\frac{\hbar(\omega_s(T)-\omega)}{k_B T}\right] + 1} \tag{A.4}$$

means the complementary probability for superelectrons being broken into normal electrons due to photonic excitation, referring to Planck's constant $\hbar$ and Boltzmann's constant k_B as well as to the pair breaking frequency $\omega_s(T)$; the latter quantity is defined by the requirement

$$\hbar\omega_s(T) = 2\Delta(T) \tag{A.5}$$

with the temperature-dependent superconductor half-gap energy $\Delta(T)$ which, for $0 \leqslant T \leqslant T_c$, obeys the approximate form

$$\Delta(T) \cong \Delta_0 \left(1 - \frac{T^3}{T_c^3}\right)^{1/4}, \tag{A.6}$$

resorting to the superconductor half-gap energy at absolute zero, Δ_0. Evidently, the particular ansatz of equations (A.3) and (A.4) derives from the notion that the probabilities under consideration should vary about $\omega_s(T)$ over a scale of frequencies corresponding to the energy of thermal fluctuations. If we suppose that the total electric current density in the superconductor is made up of the density of the supercurrent and/or the density of the normal current, with the superconducting channel being described by the London theory and the normal channel being modelled by the Drude theory [35], then

$$\sigma_{s,\nu}^{(<)}(\omega, T) = \frac{1}{\Lambda_{s,\nu}(T)}\left[\pi\delta(\omega) + \frac{\mathrm{i}}{\omega}\right] + \frac{n(T)}{n_{\mathrm{tot}}}\sigma_{s,\nu}^{(>)}(\omega, T) \tag{A.7}$$

and

$$\sigma_{s,\nu}^{(>)}(\omega, T) = \frac{\sigma_{n,\nu}(T)}{1 - \mathrm{i}\omega\tau_n(T)}, \tag{A.8}$$

where $\delta(\omega)$ stands for the Dirac delta function, $n(T)$ governs the density of the normal electrons and n_{tot} sets the density of the total of the conduction electrons. The principal components of the temperature-dependent London tensor, $\Lambda_{s,\nu}(T)$, remarked on here, are given by

$$\Lambda_{s,\nu}(T) = \frac{\Lambda_{s,\nu}^{(0)}}{1 - \frac{T^4}{T_c^4}} \tag{A.9}$$

with the respective components of the London tensor at absolute zero, $\Lambda_{s,\nu}^{(0)}$, in turn specified as

$$\Lambda_{s,\nu}^{(0)} = \frac{m_\nu}{e^2 n_{\mathrm{tot}}}, \tag{A.10}$$

or, equivalently, by the related principal components of the temperature-dependent London penetration depth, $\lambda_{s,\nu}(T)$, understanding

$$\lambda_{s,\nu}(T) = \frac{\lambda_{s,\nu}^{(0)}}{\left(1 - \frac{T^4}{T_c^4}\right)^{1/2}} \tag{A.11}$$

with the respective components of the London penetration depth at absolute zero, $\lambda_{s,\nu}^{(0)}$, in turn spelt out as

$$\lambda_{s,\nu}^{(0)} = \left(\frac{m_\nu c^2}{4\pi e^2 n_{\mathrm{tot}}}\right)^{1/2}, \tag{A.12}$$

quoting the principal components of the effective-mass tensor of the normal electrons, m_ν, and the elementary charge, e. Hence, according to the definition of the temperature-dependent London tensor or the temperature-dependent London penetration depth in terms of $n(T)$ and n_{tot}, the result

$$\frac{n(T)}{n_{\mathrm{tot}}} = \frac{T^4}{T_c^4} \tag{A.13}$$

obtains. The principal components of the tensor of static normal conductivity, $\sigma_{n,\nu}(T)$, finally read

$$\sigma_{n,\nu}(T) = \frac{e^2 n_{\mathrm{tot}} \tau_n(T)}{m_\nu}, \tag{A.14}$$

using the inverse proportionality for the scattering time of the normal electrons, $\tau_n(T)$, appropriate to very pure superconductors [34]

$$\frac{1}{\tau_n(T)} = \alpha\frac{T}{T_c} \tag{A.15}$$

with the scattering rate constant α; this requires that the condition on the range of temperature $\omega_s(T)\tau_n(T) \gg 1$ applies.

It is worth commenting that, in contrast to the predictions ensuing from the model described above, a wide maximum of the real part of the components of the tensor of dynamic electrical conductivity, $\sigma_{s,\nu}(\omega, T)$, of doubled height due to coherent electron scattering exists at frequencies far below the pair breaking frequency $\omega_s(T)$ and temperatures around $T/T_c \cong 21/25$, which a two-fluid approach, with its invaluable asset of mathematical simplicity, cannot in principle describe [36]. However, notwithstanding the fact that in this restricted frequency–temperature domain some features may be missed, the suggested model does otherwise exhibit plausible properties consistent with the general requirements on the dispersion of the dynamic electrical conductivity.

We note that the representation of the principal components of the tensor of dynamic electrical conductivity, equation (A.2), entails the asymptotic limit

$$\lim_{\omega\to\infty} 4\pi\omega\,\mathrm{Im}\,\sigma_{s,\nu}(\omega, T) = \omega_{p,\nu}^2, \tag{A.16}$$

with the respective components of the tensor of plasma frequency $\omega_{p,\nu}$ given by

$$\omega_{p,\nu} = \left(\frac{4\pi e^2 n_{\mathrm{tot}}}{m_\nu}\right)^{1/2}. \tag{A.17}$$

Applying the Kramers–Kronig dispersion relations [37] (which link the real and imaginary parts of any complex response function over the whole range of frequencies) to the general form of equation (A.1) in conjunction with equation (A.16) thus yields the sum rule for the principal components of the tensor of electric permittivity in $0 \leqslant T \leqslant T_c$:

$$\int_0^\infty \omega\,\mathrm{Im}\,\varepsilon_{s,\nu}(\omega, T)\,\mathrm{d}\omega = \frac{\pi}{2}\omega_{p,\nu}^2. \tag{A.18}$$

Of course, if our model were completely rigorous, this rule would be strictly obeyed. Indeed, in the low-temperature limit $T \to 0$, where $\tau_n(T) \to \infty$ from equation (A.15) and

$$\lim_{T\to 0} \varepsilon_{s,\nu}(\omega, T) = 1 - \frac{\omega_{p,\nu}^2}{\omega^2}\left[1 - \mathrm{i}\pi\omega\delta(\omega)\right], \tag{A.19}$$

whence the superconductor is seen to behave like a *perfect* conductor, the condition (A.18) is fulfilled identically; on the

other hand, in the high-temperature limit $T \to T_c$, where $\omega_s(T) \to 0$ from equation (A.5) with equation (A.6) and

$$\lim_{T\to T_c} \varepsilon_{s,\nu}(\omega, T) = 1 + \frac{\omega_{p,\nu}^2}{\omega^2}\left[\frac{i\omega\tau_n(T_c)}{1 - i\omega\tau_n(T_c)}\right], \qquad (A.20)$$

whence the superconductor is seen to behave like a *normal* conductor, the condition (A.18) is fulfilled identically again. Yet, for temperatures within these extremes and the values of Δ_0 and α given in table 1, our model overestimates the integral in equation (A.18), albeit merely by about 5% at most, the maximum relative deviation occurring for $T/T_c \cong 11/15$; a fact which, together with the gratification of the demand concerning the assumed material purity for temperatures virtually up to T_c, underlines the applicability of this model to superconductors that are well described in the local limit represented by the classical London approach [38].

References

[1] Joannopoulos J D, Meade R D and Winn J N 1995 *Molding the Flow of Light* (Princeton: University Press)
[2] Inoue K and Ohtaka K (ed) 2004 *Photonic Crystals: Physics, Fabrication and Applications* (Berlin: Springer)
[3] Sakoda K 2005 *Optical Properties of Photonic Crystals* (Berlin: Springer)
[4] Lopez C 2003 *Adv. Mater.* **15** 1679
[5] Okamura S, Mochiduki Y, Motohara H and Shiosaki T 2005 *Integr. Ferroelectr.* **69** 303
[6] Sychev F Y, Murzina T V, Kim E M and Aktsipetrov O A 2005 *Phys. Solid State* **47** 150
[7] Lyubchanskii I L, Dadoenkova N N, Lyubchanskii M I, Shapovalov E A and Rasing T 2003 *J. Phys. D: Appl. Phys.* **36** R277
[8] Inoue M, Fujikawa R, Baryshev A, Khanikaev A, Lim P B, Uchida H, Aktsipetrov O, Fedyanin A, Murzina T and Granovsky A 2006 *J. Phys. D: Appl. Phys.* **39** R151
[9] Lee W M, Hui P M and Stroud D 1995 *Phys. Rev.* B **51** 8643
[10] Ooi C H R and Yeung T C A 1999 *Phys. Lett.* A **259** 413
[11] Ooi C H R, Yeung T C A, Koun C H and Lim T K 2000 *Phys. Rev.* B **61** 5920
[12] Chen Y, Zhang C, Zhu Y, Zhu S and Ming N 2002 *Mater. Lett.* **55** 12
[13] Takeda H and Yoshino K 2003 *Phys. Rev.* B **67** 245109
[14] Savel'ev S, Rakhmanov A L and Nori F 2005 *Phys. Rev. Lett.* **94** 157004
[15] Wu C J, Chen M S and Yang T J 2005 *Physica* C **432** 133
[16] Takeda H, Yoshino K and Zakhidov A A 2004 *Phys. Rev.* B **70** 085109
[17] Feng L, Liu X P, Ren J, Tang Y F, Chen Y B, Chen Y F and Zhu Y Y 2005 *J. Appl. Phys.* **97** 073104
[18] Pimenov A, Loidl A, Przyslupski P and Dabrowski B 2005 *Phys. Rev. Lett.* **95** 247009
[19] Savel'ev S, Rakhmanov A L and Nori F 2006 *Physica* C **445–448** 180
[20] Berman O L, Lozovik Y E, Eiderman S L and Coalson R D 2006 *Phys. Rev.* B **74** 092505
[21] Huang H F, Mao J F, Hu Z Y, Liu J Y, Zhen D N and Yao X 2004 *J. Low Temp. Phys.* **136** 117
[22] Huang H F, Mao J F, Li X C and Li Z 2005 *IEEE Trans. Appl. Supercond.* **15** 3827
[23] Wood B and Pendry J B 2007 *J. Phys.: Condens. Matter* **19** 076208
[24] Ozbaya E, Temelkuran B, Sigalas M, Tuttle G, Soukoulis C M and Ho K M 1996 *Appl. Phys. Lett.* **69** 3797
[25] Tsurumachi N, Abe M, Arakawa M, Yoda T, Hattori T, Qi J, Masumoto Y and Nakatsuka H 1999 *Japan. J. Appl. Phys.* **38** L1400
[26] Wang X Z 2005 *J. Phys.: Condens. Matter* **17** 5447
[27] Kuchko A N, Sokolovskii M L and Kruglyak V V 2005 *Physica* B **370** 73
[28] Lyubchanskii I L, Dadoenkova N N, Lyubchanskii M I, Shapovalov E A, Zabolotin A E, Lee Y P and Rasing T 2006 *J. Appl. Phys.* **100** 096110
[29] Landau L D and Lifshitz E M 1995 *Classical Theory of Fields* (Oxford: Elsevier)
[30] Rauh H and Stoneham A M 1984 *J. Phys. A: Math. Gen.* **17** 3299
[31] Plecenik A, Benacka S, Darula M, Chromik S, Mikusík P and Grajcar M 1991 *Solid State Commun.* **78** 809
[32] Tanner D B, Herr S L, Kamarás K, Porter C D, Tache N, Etemad S, Venkatesan T, Inam A, Wu X D, Hegde M S and Dutta B 1990 *Low-Dimensional Conductors and Superconductors* ed S Barisic and E Tutis (Zagreb: Fizika) p 205
[33] Friedmann T A, Rabin M W, Giapintzakis J, Rice J P and Ginsberg D M 1990 *Phys. Rev.* B **42** 6217
[34] Tanner D B and Timusk T 1992 *Physical Properties of High-Temperature Superconductors* vol III, ed D M Ginsberg (Singapore: World Scientific) p 363
[35] Orlando T P and Delin K A 1991 *Foundations of Applied Superconductivity* (New York: Addison-Wesley)
[36] Tinkham M 2004 *Introduction to Superconductivity* (New York: Dover)
[37] Landau L D, Lifshitz E M and Pitaevskii L P 1995 *Electrodynamics of Continuous Media* (Oxford: Elsevier)
[38] Waldram J R 1996 *Superconductivity of Metals and Cuprates* (Bristol: Institute of Physics Publishing)